

Development of a polymer resin immobilized catalysts for the oxidative transformation of ethylbenzene

Sunil Kumar¹, Praveen Kumar Gupta^{1*}, Amit Kumar² and Ramesh Kumar³

¹Department of Chemistry, Maharishi Markandeshwar (Deemed to be University), Mullana 133207, Haryana, India

²Department of Chemistry, Indira Gandhi National College, Ladwa, Kurukshetra 136132, Haryana, India

³Department of Chemistry, Kurukshetra University, Kurukshetra, Haryana 136119, India

*Authors to whom correspondence should be addressed:

Department of Chemistry
Maharishi Markandeshwar (Deemed to be University)
Mullana 133207, Haryana
India

Email: parveen.gupta@mmumullana.org;
ORCID ID: <https://orcid.org/0000-0002-2718-1310>

This article has been accepted for publication and undergone full peer review but has not been through the copyediting, typesetting, and proofreading process, which may lead to differences between this version and the official version of record.

Please cite this article as: Kumar S., Gupta P.K., Kumar A., Kumar R. Development of a polymer resin immobilized catalysts for the oxidative transformation of ethylbenzene. *Mongolian Journal of Chemistry*, 27(55), 2026, xx-xx

<https://doi.org/10.5564/mjc.v27i55.4288>

1 Development of a polymer resin immobilized catalysts for the oxidative 2 transformation of ethylbenzene

3
4 Sunil Kumar¹, <https://orcid.org/0009-0008-5417-3034>

5 Praveen Kumar Gupta^{1*}, <https://orcid.org/0000-0002-2718-1310>

6 Amit Kumar², <https://orcid.org/0009-0000-2748-1543>

7 Ramesh Kumar³, <https://orcid.org/0000-0003-2089-2213>

8
9 ¹Department of Chemistry, Maharishi Markandeshwar (Deemed to be University), Mullana 133207,
10 Haryana, India

11 ²Department of Chemistry, Indira Gandhi National College, Ladwa, Kurukshetra 136132, Haryana,
12 India

13 ³Department of Chemistry, Kurukshetra University, Kurukshetra, Haryana 136119, India

14

15 ABSTRACT

16 New copper, manganese and vanadium based heterogeneous catalysts have been
17 developed by the immobilization of pyridyl benzimidazole onto the polymer support. The
18 active catalysts were characterized using CHN, FT-IR, DRS, EPR, AAS and EDX techniques
19 and successfully used for the oxidative transformation of ethyl benzene. Metal loading in
20 mmol per gram of resin in different catalysts was found to be 0.94-1.34. The catalytic
21 potential of the synthesized catalysts was evaluated for the oxidation of ethylbenzene using
22 hydrogen peroxide and *tert*-butyl hydroperoxide as oxidant with undiminished efficiency
23 profiles and good reusability (up to four cycles). Notably, no metal contamination in the final
24 products was observed. The comparative evaluation revealed that the highest percentage
25 conversion (82.8 %) and highest selectivity (82.5) for benzaldehyde formation was attained
26 with manganese as catalyst using H₂O₂ as an oxidant. The mechanism of the oxidation of
27 ethylbenzene in the presence of catalyst has also been proposed. The developed catalytic
28 systems are operationally simple and environmentally clean.

29 **Keywords:** Heterogeneous catalyst, recyclability, chloromethylated polystyrene,
30 ethylbenzene, 2-(2-pyridyl) benzimidazole, oxidants, selectivity.

35

36 **INTRODUCTION**

In context to modern ecosystem the development of efficient and sustainable catalytic systems for the oxidation of hydrocarbons, such as ethylbenzene, is of paramount importance in both industrial and environmental contexts [1]. Traditional oxidation methods often suffer from drawbacks such as harsh reaction conditions, low selectivity, and the use of environmentally harmful oxidants [2]. Consequently, there is a growing demand for catalysts that can operate under mild conditions, exhibit high selectivity, and are environmentally benign [3]. In this regard, supported catalysts have emerged as a promising class of catalysts, combining the advantages of homogeneous catalysis, such as high activity and selectivity, with the stability and recyclability of heterogeneous systems [4]. Chloromethylated polymers, in particular, have gained significant attention as versatile supports due to their ease of functionalization and ability to anchor a wide range of ligands and metal centres [5-6]. When paired with redox-active transition metals, these polymer-supported systems exhibit enhanced catalytic performance in various chemical transformations like oxidation [7-8], hydrogenation [9], esterification [10], carbonylation [11], olefinations [12], olefin metathesis [13], isomerisation [14], cross coupling reactions [15] etc. The 2-(2-pyridyl) benzimidazole ligand [16-17], known for its strong chelating ability and stability, has been widely used to form well-defined complexes with diverse catalytic applications. By supporting 2-(2-pyridyl) benzimidazole based complexes onto chloromethylated polymers, it is possible to create robust and recyclable catalysts with tailored properties for oxidation reactions. This research focuses on the synthesis of new immobilized 2-(2-pyridyl) benzimidazole based metal catalysts. The study aims to explore the structural and spectroscopic characteristics of these catalysts, as well as their catalytic efficiency, selectivity, and reusability in the oxidative transformation of ethylbenzene. By utilizing the synergistic effects of the 2-(2-pyridyl) benzimidazole ligand, the redox-active metal centres, and the polymer support, this work seeks to develop a sustainable and efficient catalytic system for the oxidation of aromatic hydrocarbon. The oxidation of ethylbenzene in the presence of catalyst can produce a range of products, including benzaldehyde, acetophenone and phenylacetic acid as a major product [18-19]. Benzaldehyde is a versatile organic compound with a distinctive odor and a wide range of applications across various industries. It is the simplest aromatic aldehyde and serves as a key intermediate in the synthesis of numerous chemicals, widely used as a flavoring agent in foods and beverages due to its characteristic almond-like aroma and also finds uses as a

69 key component in almond extracts [20]. Acetophenone is an important organic compound
70 with several applications in various industries. It is primarily known for its use as a flavoring
71 agent, fragrance, and intermediate in chemical synthesis [21]. Phenylacetic acid is used in
72 the synthesis of several pharmaceuticals, it is a precursor in the production of some β -lactam
73 antibiotics like penicillin and ampicillin, which are critical for treating bacterial infections, used
74 in drug formulations and synthesizing compounds for anti-inflammatory, anticancer, and
75 other therapeutic purposes [22].

76 EXPERIMENTAL

77 **Materials and instruments:** Chloromethylated polystyrene (crosslinked with
78 divinylbenzene) was obtained as gift from Thermax Chemical Limited Pune. 2-(2-pyridyl)
79 benzimidazole (Sigma-aldrich); vanadyl sulphate pentahydrate, copper chloride dihydrate,
80 manganese acetate tetrahydrate, silver nitrate, dimethylformamide, conc. nitric acid,
81 hydrogen peroxide (H_2O_2 , 30%), *tert*-butyl hydroperoxide (70%), acetonitrile,
82 dimethylformamide, ethanol and methanol (CDH) were used for the synthesis. The Fourier
83 Transform Infrared (FT-IR) spectra were recorded on Shimadzu IR spirit fourier transform
84 infrared spectrophotometer. The diffused reflectance spectra (DRS) of the samples were
85 recorded from UV-2600 Shimadzu double-beam spectrophotometer using $BaSO_4$ as the
86 standard. Energy-dispersive X-ray analyses (EDX) spectra were recorded in FEG scanning
87 electron microscope Hitachi SU8010 Series; CHNS were recorded on Thermo Scientific
88 flash 2000; Metal analyses were performed on Shimadzu ASC-6880 atomic absorption
89 spectrophotometer (AAS). EPR spectra were recorded on JES-FA200 X-band (9.45 GHz)
90 spectrometer with a modulation frequency of 100 kHz. Modulation amplitude typically set at
91 2.0 Gauss, to maximize the signal without affecting resolution. GC-MS analysis were
92 conducted on an Agilent 7000 GC/TQ system with a GsBP-624 column and Flame ionisation
93 detector (FID) detector-equipped gas chromatograph.

94 **Functionalization of polystyrene resin with 2-(2-pyridyl) benzimidazole (PSCH₂-PBZ):**
95 The synthesis of the functionalized resin began by swelling 1 g of chloromethylated
96 polystyrene in 20 mL of DMF at room temperature for 1 h. Separately, 4.5 mmol of 2-(2-
97 pyridyl) benzimidazole was dissolved in 20 mL of DMF and subsequently added to the pre-
98 swollen polymer suspension. Upon addition, the solution's color rapidly changed to light
99 yellow. To facilitate the reaction, 0.7 mL of triethylamine was introduced, and the mixture
100 was refluxed under stirring at 80 °C for 8 h. After completion, the reaction mixture was
101 allowed to cool to room temperature, followed by vacuum filtration. The product was

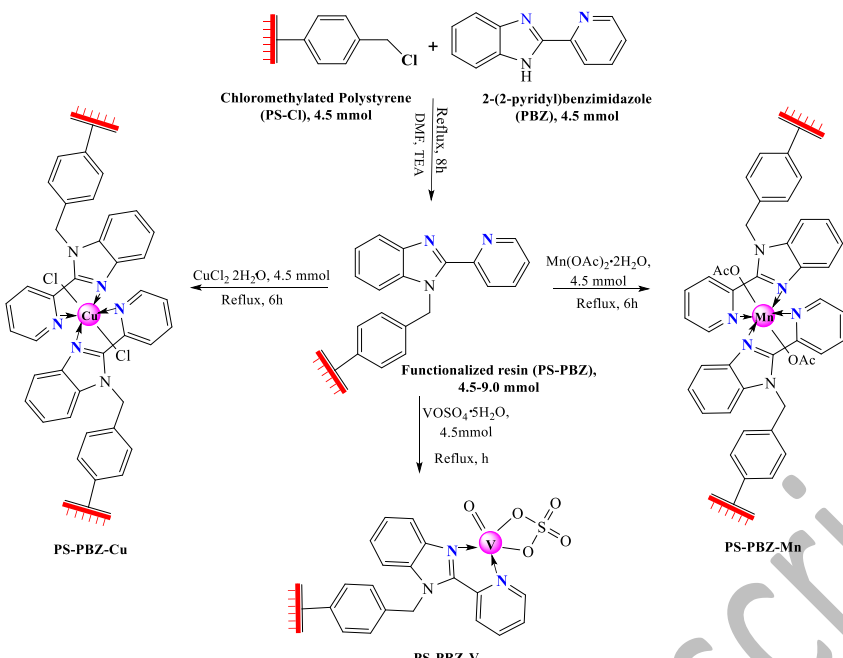
102 thoroughly washed multiple times with hot DMF and hot ethanol to remove any unreacted
103 residues. Finally, the functionalized resin was dried in an air oven at 80 °C.

104 **Loading of metal (V/Mn/Cu) on functionalized resin:** 1.0 g sample of PSCH₂-PBZ was
105 swelled in 10 mL of DMSO for 1 h. A solution of CuCl₂·2H₂O/ VOSO₄·5H₂O/
106 Mn(CH₃COO)₂·4H₂O (4.5-9.0 mmol) was prepared in DMSO and subsequently added to the
107 swelled polymer suspension. As the reaction progressed, a noticeable change in the resin's
108 color was observed. The mixture was then refluxed under continuous stirring for 6 h. After
109 completion, the resin was allowed to cool to room temperature, followed by vacuum filtration.
110 It was then thoroughly washed multiple times with hot DMSO and hot ethanol to remove any
111 unreacted species. Finally, the purified metal loaded resin was dried in an oven at 80°C.

112 **Catalytic oxidation reaction:** The oxidation reaction was performed in a thermostatted
113 oil bath using a round-bottom flask. The catalyst was pre-swollen in acetonitrile (20 ml) for
114 30 minutes before adding ethylbenzene (10 mmol), an oxidant (20 mmol), and the catalyst
115 (0.1–0.15 g). The mixture was refluxed and the reaction was primarily examined on TLC
116 under the varying conditions such as catalyst amount, oxidant type (TBHP, H₂O₂),
117 temperature, and duration (4–8 h). The products were confirmed by GC-MS.

118 RESULTS AND DISCUSSION

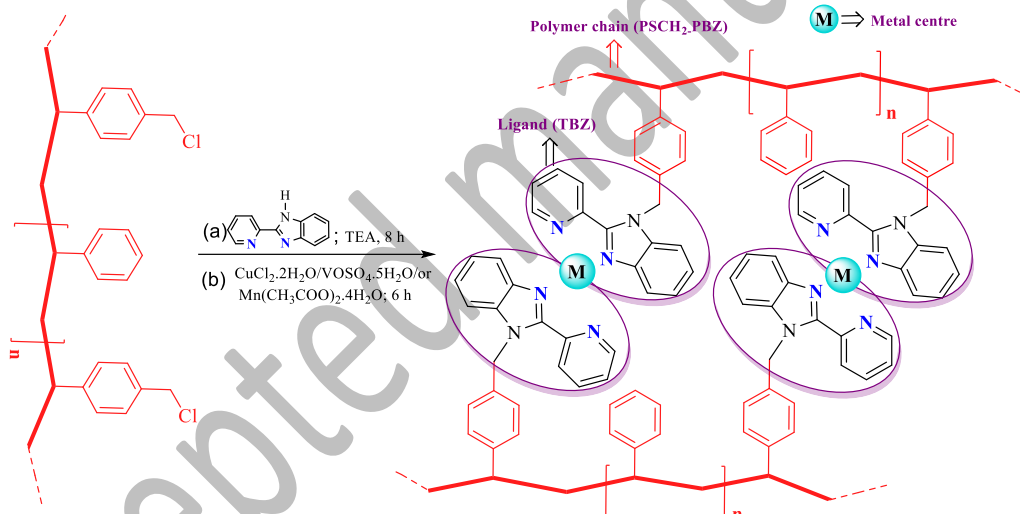
119 The crosslinked polystyrene resin was functionalized with 2-(2-pyridyl) benzimidazole
120 using triethylamine and DMF, forming [PSCH₂-PBZ] (**Scheme 1**). Ligand attachment was
121 confirmed by heating the beads with pyridine, followed by nitric acid and silver nitrate,
122 where no white precipitate indicated chlorine replacement. The ligand's para-position
123 attachment is shown in **Fig. 1**. Metal loading onto the functionalized resin (**Scheme 2**) was
124 initially confirmed by a color change and later by spectroscopic analysis.



125

126

127

Scheme 1. Synthesis of functionalized resin and its metal catalyst

128

129
130**Fig. 1.** Picture illustrating the metal loaded polystyrene beads (neglecting the cross-linking with divinylbenzene)131
132
133
134
135
136
137
138
139

Characterization: Elemental data for the functionalised resin and its metal catalysts are presented in **Table 1**. Metal content was determined experimentally by acid leaching of 0.1 gm of the catalyst for 3 h followed by AAS determination. The experiments were performed at least three times, and the mean values are reported in **Table 1**. Ligand incorporation was calculated from %N obtained from CHN analyser. Ligand incorporation (mmol/g) = % N × 100 / (14 × n), where n is the number of nitrogen atoms per ligand. Metal incorporation was calculated using the formula: Metal incorporation (mmol/g) = Observed metal % × 10/Atomic weight of metal. From these data, loading of ligand and metal onto the polystyrene resin was determined

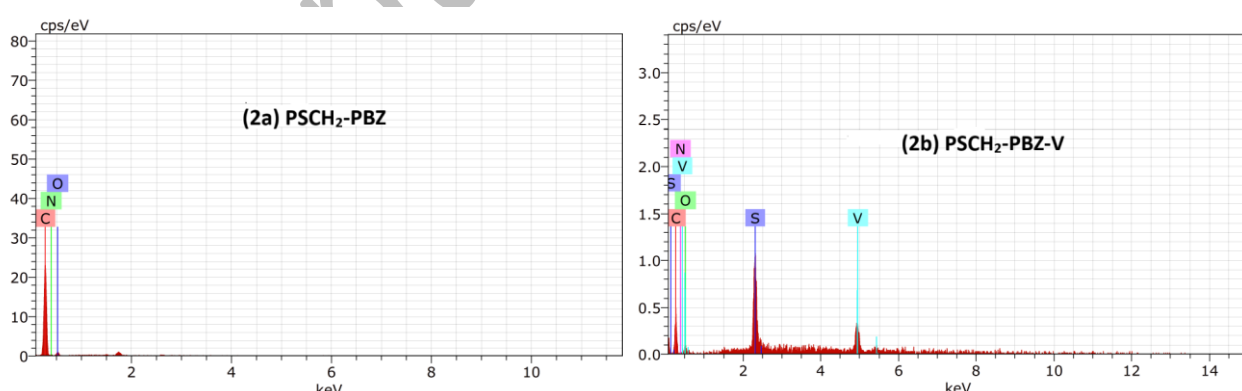
140 which helps in evaluating the ligand to metal stoichiometry.

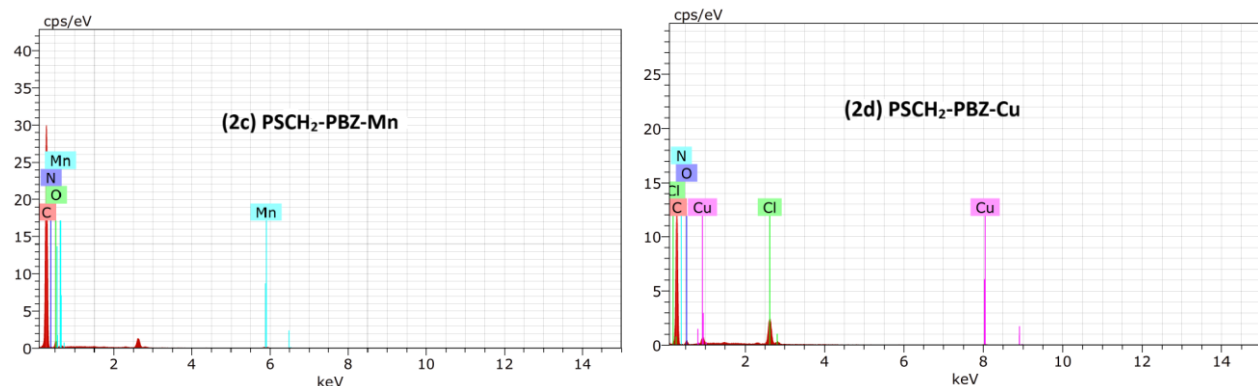
141 **Table 1.** Analytical data of PSCH₂-PBZ and its metal catalyst

	Colour	Elemental analysis (%)					Ligand incorporation (mmol per gram of resin)	Metal incorporation (mmol per gram of resin) (Mean of triplicates)	Ligand :Metal ratio
		C	H	N	S	M			
[PSCH ₂ -PBZ]	off white	82.52	7.17	10.31			2.45		
[PSCH ₂ -PBZ-V]	light green	60.38	5.02	7.01	5.77	6.81	1.67	1.37, 1.32, 1.33 → 1.34	1.2:1
[PSCH ₂ -PBZ-Mn]	Brown	72.82	6.32	8.64			5.65	2.05	1.05, 1.03, 1.01 → 1.03
[PSCH ₂ -PBZ-Cu]	light yellow	71.89	5.93	8.80			5.97	2.1	0.92, 0.94, 0.96 → 0.94

142 The successful attachment of the ligand onto the polystyrene resin, followed by metal
 143 loading, was verified using EDX analysis (**Fig. 2**). The spectrum of [PSCH₂-PBZ] (**2a**)
 144 displays signals corresponding to C and N, confirming the ligand's incorporation with the
 145 polymer. The detection of metal ion signals across all catalysts indicates effective metal
 146 binding with [PSCH₂-PBZ]. The EDX spectrum of [PSCH₂-PBZ-V] (**2b**) displays
 147 characteristic signals corresponding to C, N, O, S, and V elements. The presence of oxygen
 148 and sulphur peaks confirms the coordination of sulphate group to the metal centre. The
 149 [PSCH₂-PBZ-Mn] (**2c**) catalyst exhibits signals due to C, N, O, and Mn, where the oxygen
 150 signal supports the coordination of acetate group. Similarly, the EDX spectrum of [PSCH₂-
 151 PBZ-Cu] (**2d**) shows peaks for C, N, Cl, and Cu, and the presence of chlorine indicates the
 152 coordination of chloride ions with the copper centre.

153

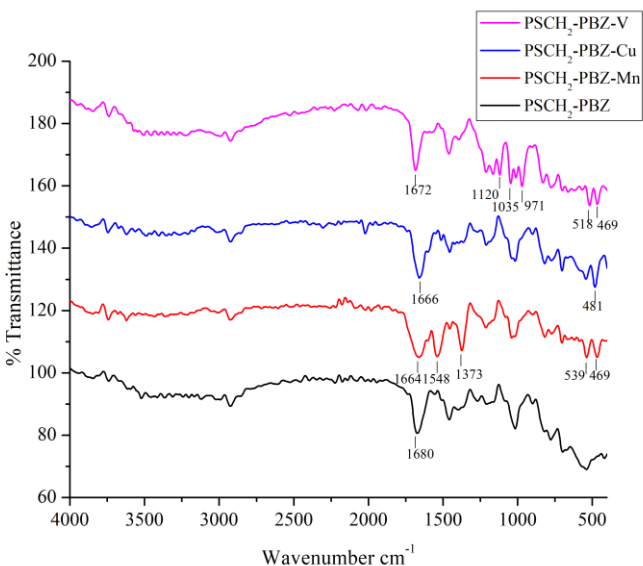




154

155 **Fig. 2(a-d).** EDX plot of functionalized polymer and polymer supported metal catalysts156 **FT-IR Study**

157 The overlay spectra of the synthesized compounds are presented in **Fig. 3**, while **Table 2**
 158 summarizes the key vibrational bands observed for the supported 2-(2-pyridyl)
 159 benzimidazole [PSCH₂-PBZ] and its corresponding metal catalysts. In the spectrum of
 160 [PSCH₂-PBZ], the absorption bands at 1680 cm⁻¹ and 1264 cm⁻¹ can be attributed to the
 161 stretching vibrations of the ν (C=N) (imi + py) bonds (from both imidazole and pyridine rings)
 162 and the C-N bond, respectively. A comparative analysis of the FT-IR spectra of [PSCH₂-
 163 PBZ] and its catalysts indicates that the ligand coordinates to the metal ions in a bidentate
 164 manner. This is evident from the significant shifts in the C=N stretching frequencies, which
 165 vary by approximately 8-16 cm⁻¹ in the metal complexes, confirming the involvement of
 166 nitrogen atoms in coordination [23]. However, the C-N stretching frequency in the polymer-
 167 supported ligand remains largely unchanged upon metal coordination. Further evidence of
 168 metal binding is provided by the appearance of new bands in the metal catalysts,
 169 corresponding to metal-nitrogen (M-N), metal-oxygen (M-O), and metal-chlorine (M-Cl)
 170 interactions. These bands are observed in the regions of 469-481 cm⁻¹, 518-539 cm⁻¹, and
 171 365 cm⁻¹, respectively. In the case of [PSCH₂-PBZ-Mn], distinct bands at 1548 cm⁻¹ and
 172 1373 cm⁻¹ can be linked to the asymmetric and symmetric stretching vibrations of the acetate
 173 (OAc) groups, suggesting their monodentate coordination and supporting the covalent
 174 nature of the metal-oxygen bond [24]. Additionally, in [PSCH₂-PBZ-V], a characteristic band
 175 at 971 cm⁻¹ confirms the presence of a V=O stretching mode [25]. Furthermore, absorption
 176 band observed at 1120 cm⁻¹ and 1035 cm⁻¹ is associated with bidentate sulfate coordination,
 177 as indicated by the asymmetric and symmetric stretching vibrations of the SO₄ group [26].



178

179 **Fig. 3.** Overlap spectra of functionalized polymer and polymer supported metal catalysts180 **Table 2.** FTIR data for the PSCH₂-TBZ and its complexes

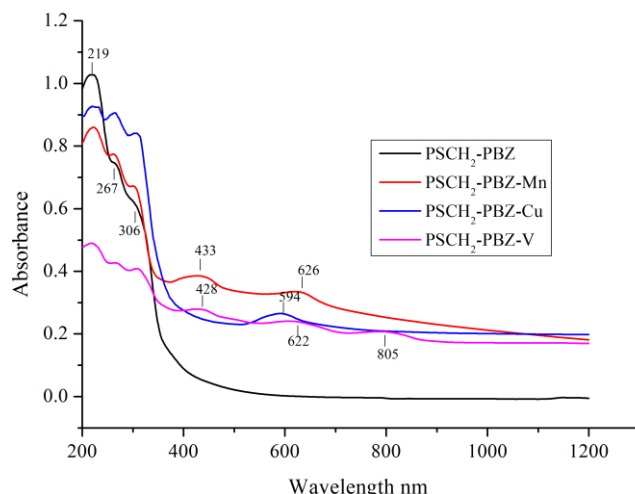
Polymer-supported compounds	$\nu(C=N)(imi + py)$	$\nu(C-N)$	$\nu_{sy}(OAc)/\nu_{asy}(OAc)$	$\nu_{sy}(SO_4)/\nu_{asy}(SO_4)$	$\nu(V=O)$	$\nu(M-N)$	$\nu(M-O)$	$\nu(M-Cl)$
[PSCH₂-PBZ]	1680	1264						
[PSCH₂-PBZ-V]	1672	1262		1120, 1035	971	469	518	
[PSCH₂-PBZ-Mn]	1664	1263	1548, 1373			469	539	
[PSCH₂-PBZ-Cu]	1666	1264				481		365

181

182 **Diffused reflectance spectra**

183 The diffused reflectance spectroscopy (DRS) analysis was conducted (**Table 3 and Fig. 4**)
 184 to investigate the electronic transitions and coordination environments of the catalysts. This
 185 technique provided information to confirm the oxidation states and geometries of the metal
 186 centres. The DRS spectrum of the ligand-functionalized polymer exhibited distinct
 187 absorption bands at 45662, 38167 and 32680 cm^{-1} , corresponding to $\phi \rightarrow \phi^*$, $\pi \rightarrow \pi^*$, $n \rightarrow$
 188 π^* transitions within the 2-(2-pyridyl) benzimidazole ligand. These bands remained present
 189 in the metal-loaded catalysts, with slight shifts, indicating successful coordination of the
 190 metal centers without significant alteration of the polymer's electronic structure. The
 191 vanadium-supported catalyst displayed three well-defined d-d transition bands at 12422;
 192 16077 and 24331 cm^{-1} . These transitions were characteristic of a five-coordinate
 193 oxovanadium (IV) species in a square pyramidal (C_{4v}) geometry. The observed bands were
 194 assigned to the electronic transitions $^2\text{B}_2 \rightarrow ^2\text{E}$, $^2\text{B}_2 \rightarrow ^2\text{B}_1$ and $^2\text{B}_2 \rightarrow ^2\text{A}_1$, consistent with
 195 previously reported spectral parameters for similar oxovanadium complexes [27-28]. The
 196 manganese catalyst exhibited absorption bands at 15974 and 23094 cm^{-1} , corresponding to
 197 the spin-allowed $^2\text{B}_{1g} \rightarrow ^2\text{A}_{1g}$, $^2\text{B}_{1g} \rightarrow ^2\text{B}_{2g}$, $^2\text{B}_{1g} \rightarrow ^2\text{E}_g$ transitions, respectively. These

198 transitions confirmed the presence of high-spin Mn (II) in an octahedral ligand field [29-30].
 199 The copper catalyst exhibited a broad absorption band centred around 16835 cm^{-1} ,
 200 indicative of multiple overlapping d-d transitions. These bands were assigned to $^2\text{B}_{1\text{g}} \rightarrow ^2\text{A}_{1\text{g}}$,
 201 $^2\text{B}_{1\text{g}} \rightarrow ^2\text{B}_{2\text{g}}$, $^2\text{B}_{1\text{g}} \rightarrow ^2\text{E}_{\text{g}}$ transitions, which are characteristic of Cu (II) complexes in a
 202 distorted octahedral ($\text{D}_{4\text{h}}$) symmetry [29, 31]. The broad nature of the absorption band was
 203 attributed to Jahn-Teller distortion, a well-known effect in Cu (II) systems that influences
 204 their electronic structure.



205
 206 **Fig.4.** Overlap DRS spectra of functionalized polymer its metal catalysts
 207

208 **Table 3.** Diffused Reflectance spectral data of functionalized resin and its metal catalysts

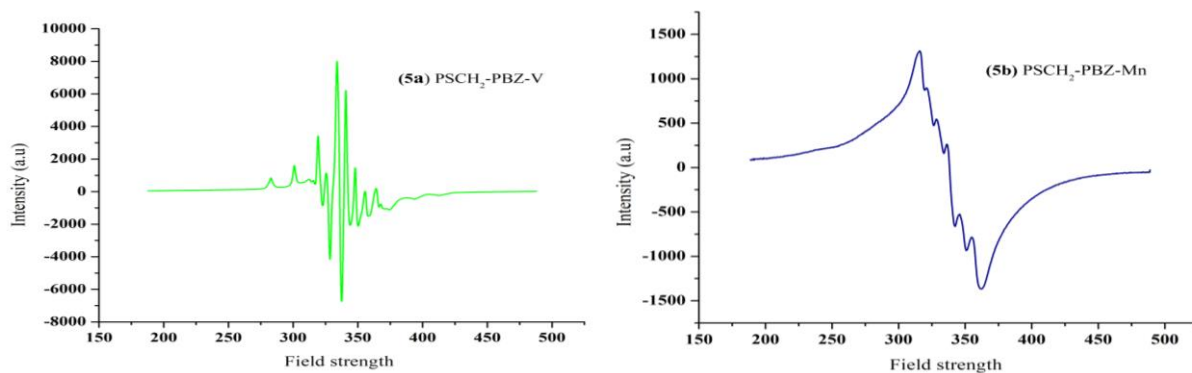
Polymer supported metal catalysts	Transitions (cm^{-1})	Band assignment
[PSCH ₂ -PBZ]	45662, 38167, 32680	$\varphi \rightarrow \varphi^*$, $\pi \rightarrow \pi^*$, $\text{n} \rightarrow \pi^*$
[PSCH ₂ -PBZ-V]	12422; 16077; 24331	$^2\text{B}_2 \rightarrow ^2\text{E}$; $^2\text{B}_2 \rightarrow ^2\text{B}_1$; $^2\text{B}_2 \rightarrow ^2\text{A}_1$
[PSCH ₂ -PBZ-Mn]	15974; 23094	$^6\text{A}_{1\text{g}} \rightarrow ^4\text{T}_{1\text{g}}(\text{G})$; $^6\text{A}_{1\text{g}} \rightarrow ^4\text{T}_{2\text{g}}(\text{G})$
[PSCH ₂ -PBZ-Cu]	16835	$^2\text{B}_{1\text{g}} \rightarrow ^2\text{A}_{1\text{g}}$; $^2\text{B}_{1\text{g}} \rightarrow ^2\text{B}_{2\text{g}}$; $^2\text{B}_{1\text{g}} \rightarrow ^2\text{E}_{\text{g}}$

209

210 EPR Study

211 The electron spin resonance (ESR) spectra (**Fig. 5**) of the vanadium and manganese
 212 catalysts were recorded at room temperature to gain insight into their electronic
 213 environments and coordination geometries. This technique provided valuable information
 214 regarding the oxidation states, ligand interactions, and overall structural properties of the
 215 metal centers within the immobilized catalysts. The ESR spectrum of the vanadium-based
 216 catalyst displayed a distinct anisotropic signal characteristic of vanadyl species (VO^{2+}),
 217 confirming the presence of V(IV) in a square pyramidal coordination environment. The
 218 hyperfine splitting pattern, arising from the interaction between the unpaired electron and

219 the vanadium nucleus ($I = 7/2$), resulted in an eight-line signal. The calculated g-values, $g_{\parallel} = 1.98$ and $g_{\perp} = 2.0$, along with the hyperfine coupling constants $A_{\parallel} = 178$ G and $A_{\perp} = 80$ G, 220 were indicative of a typical C_{4v} symmetry. The obtained spectral parameters confirmed that 221 the vanadium centre was coordinated in a manner consistent with the expected 222 oxovanadium complexes, with the V=O bond oriented along the principal axis [32-33]. In the 223 case of the manganese catalyst, the ESR spectrum exhibited a characteristic six-line 224 hyperfine splitting pattern, typical of Mn (II) species ($I = 5/2$). The well-defined hyperfine 225 interactions confirmed the presence of high-spin Mn (II) centers within the polymer 226 framework. The g-value of $g = 2.02$ and hyperfine coupling constant $A = 77$ G suggested 227 that the manganese ions were in an octahedral ligand field [34-35]. The manganese catalyst 228 displayed well resolved signal patterns due to spin-exchange interactions between 229 neighboring Mn (II) centers, indicating a stable coordination environment without significant 230 distortion.



232
233 **Fig. 5(a-b).** EPR plot of $[\text{PSCH}_2\text{-PBZ-V}]$ and $[\text{PSCH}_2\text{-PBZ-Mn}]$

234 **Catalytic activity**

235 The catalytic efficiency of the synthesized polymer-supported metal catalysts was 236 systematically assessed for the oxidation of ethylbenzene. The progress of the reaction was 237 checked by taking small samples at different time intervals and analyzing them initially by 238 TLC and finally by gas chromatography. The product selectivity and conversion of 239 ethylbenzene were calculated using GC-MS. Each experiment was repeated at least three 240 times, and average values are reported. The conversion and selectivity values were 241 obtained using the relative peak areas in the GC-MS chromatograms:

242 % Conversion = $(\sum \text{area of all products} \div \sum \text{area of substrate + products}) \times 100$.

243 % Selectivity = $(\text{Area of a particular product} \div \sum \text{area of all products}) \times 100$.

244 Samples of the solution were also tested for metal content at regular intervals. No metal was 245 found in the solution, showing that the catalyst metal did not leach out during the reaction. 246 After three reuse cycles, only a small decrease in metal content was observed. The study

247 primarily focused on understanding the influence of different parameters, including oxidant
248 type, reaction duration, temperature, and catalyst loading, to achieve optimal reaction
249 conditions. Benzaldehyde was identified as the major product, accompanied by minor
250 amounts of acetophenone and phenylacetic acid.

251 **Optimization of Oxidants**

252 To determine the most effective oxidant for the reaction, both hydrogen peroxide (H_2O_2) and
253 tert-butyl hydroperoxide (TBHP) were employed under identical conditions. Control
254 experiments performed in the absence of an oxidant confirmed that no significant conversion
255 occurred, establishing the necessity of an oxidative environment. The results demonstrated
256 that (**Table 4 & 5**), H_2O_2 exhibited superior efficiency in acetonitrile in terms of percentage
257 conversion (82.8%) and selectivity (82.5%) towards benzaldehyde, particularly in the
258 presence of manganese-supported catalysts.

259 **Influence of Reaction Temperature**

260 Temperature variation significantly impacted ethylbenzene oxidation. Experiments
261 conducted between 40 °C to 80 °C revealed a direct correlation between temperature and
262 conversion rate up to an optimal value of 65 °C. Beyond this temperature, peroxide
263 decomposition increased, leading to reduced efficiency. Thus, 65 °C was identified as the
264 ideal temperature for maximizing both conversion and selectivity.

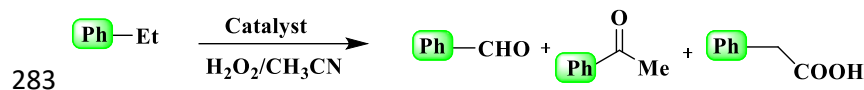
265 **Effect of Reaction Time**

266 The oxidation progress was monitored over time, revealing a gradual increase in
267 ethylbenzene conversion. The reaction progress was monitored by conducting ethyl
268 benzene reactions with TBHP/ H_2O_2 in 1:2 ratio. An induction period of approximately 2 h
269 was observed, followed by a steady increase in product formation. The highest conversion
270 rates were achieved after 7 h (**Fig. 6**), with no significant improvement beyond this point.
271 Importantly, product selectivity remained consistent throughout extended reaction times,
272 suggesting minimal side reactions.

273 **Catalyst Loading and Efficiency**

274 The impact of catalyst concentration was evaluated by varying the catalyst amount from 0.1
275 g to 0.15 g, keeping the ethylbenzene and TBHP/or H_2O_2 conc. in 1:2 ratio, temperature 65
276 °C and time 4-8 h. The influence of the amount of catalyst on the oxidation of ethylbenzene
277 as a function of time is shown in **Table 4-5 and Fig. 6(a-d)**. In the absence of a catalyst,
278 only a negligible reaction was observed (6.2% to 12.8%). Increasing the catalyst
279 concentration enhanced the conversion rate due to the greater availability of active sites.

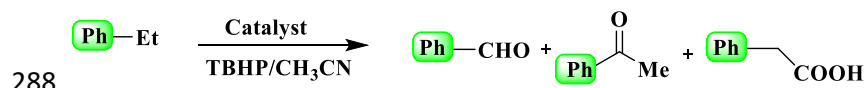
280 However, beyond 0.15 g, no substantial improvement was noted, indicating that saturation
 281 was reached.

282 **Table 4.** Conversion of ethylbenzene and Product Selectivity

Catalyst	Amount of catalyst (g)	Time (h)	Conversion (%)	Selectivity (%)			
							Others
Blank test	0.1	4	6.2	75.6	18.5	3.3	2.6
		5	7.7	76.2	17.6	3.6	2.6
		6	8.9	76.5	17.7	3.3	2.5
		7	11.1	77.4	17.8	2.6	2.2
	0.15	8	11.1	77.5	17.3	2.6	2.6
		4	55.1	80.7	13.7	3.1	2.5
		5	58.3	81.3	12.5	3.6	2.6
		6	63.5	79.9	14.3	3.1	2.7
[PSCH ₂ -TBZ-V]	0.1	7	70.3	81.8	13.5	3.1	1.6
		8	70.3	81.8	13.5	3.1	1.6
		4	56.2	81.7	12.4	3.5	2.4
		5	59.9	80.4	14.7	3.6	1.3
	0.15	6	67.2	79.1	13.9	4.0	3.0
		7	74.4	80.2	12.7	4.8	2.3
		8	74.4	80.2	12.7	4.8	2.3
		4	49.9	82.5	11.3	3.7	2.5
[PSCH ₂ -TBZ-Mn]	0.1	5	56.2	81.7	12.8	3.3	2.2
		6	65.1	82.4	11.3	4.7	1.6
		7	75.7	82.0	10.8	4.8	2.4
		8	75.7	82.0	10.8	4.8	2.4
	0.15	4	56.1	80.8	12.2	5.8	1.6
		5	68.7	82.5	10.2	4.9	2.5
		6	73.6	80.9	11.1	5.8	2.4
		7	82.8	80.0	11.8	4.6	3.6
[PSCH ₂ -TBZ-Cu]	0.1	8	82.8	80.0	11.8	4.6	3.6
		4	42.0	75.5	17.7	4.6	2.2
		5	45.2	76.8	18.7	3.4	1.1
		6	49.5	75.6	17.1	4.7	2.6
	0.15	7	52.8	74.4	18.8	4.8	2.0
		8	52.8	74.4	18.8	4.8	2.0
		4	43.5	76.8	17.9	3.1	2.2
		5	46.1	75.2	18.6	4.7	1.5
[PSCH ₂ -TBZ-Cu]	0.15	6	51.2	74.2	18.6	4.5	2.7
		7	55.5	75.8	20.1	3.1	1.0
		8	55.5	75.8	20.1	3.1	1.0

284 *Reaction conditions: CH₃CN (20 ml), Ethylbenzene (10 mmol), H₂O₂ (20 mmol), Temperature (65 °C); Conversion refers to
 285 GCMS analysis.

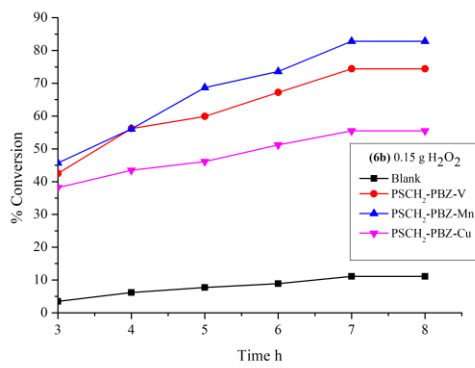
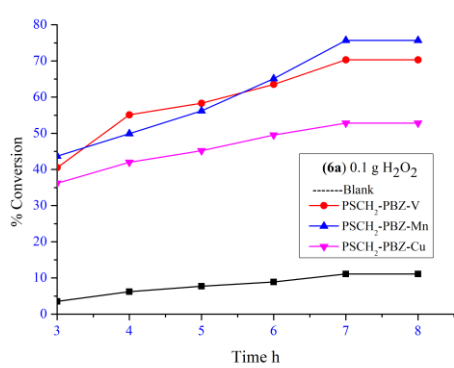
286

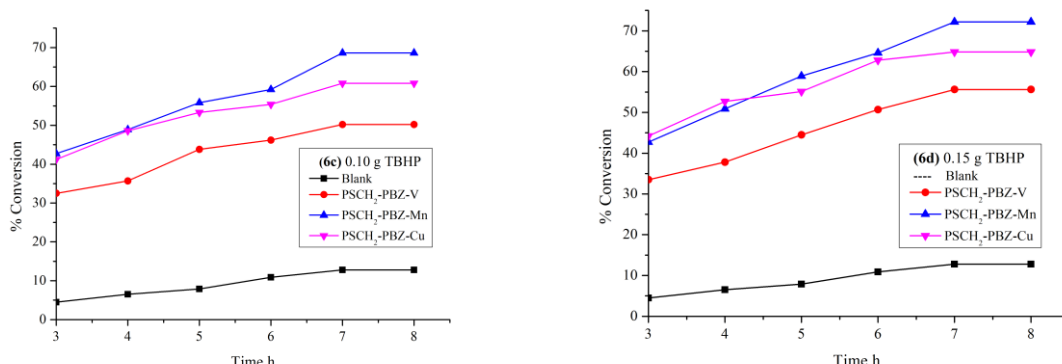
287 **Table 5.** Conversion of ethylbenzene and Product Selectivity

Catalyst	Amount of catalyst (g)	Time (h)	Conversion (%)	Selectivity (%)			
							Others

Blank test		4	6.5	72.6	19.5	4.2	2.7
		5	7.9	70.8	20.5	4.2	2.7
		6	10.9	70.6	20.2	4.8	2.4
		7	12.8	71.8	18.9	3.6	1.6
		8	12.8	71.8	18.9	3.6	1.6
[PSCH ₂ -TBZ-V]	0.1	4	35.7	72.7	17.1	7.4	2.8
		5	43.8	74.3	17.0	6.4	2.3
		6	46.2	72.2	18.2	6.2	3.4
		7	50.2	77.1	15.1	5.6	2.2
		8	50.2	77.1	15.1	5.6	2.2
	0.15	4	37.8	69.5	20.6	7.4	2.5
		5	44.5	71.5	18.6	7.6	2.3
		6	50.7	72.0	20.5	5.0	2.5
		7	55.6	71.4	19.6	6.5	2.5
		8	55.6	71.4	19.6	6.5	2.5
[PSCH ₂ -TBZ-Mn]	0.1	4	48.9	78.5	12.4	5.4	3.7
		5	55.8	80.3	11.2	6.2	2.3
		6	59.2	78.5	10.5	8.1	2.9
		7	68.6	78.6	11.5	7.5	2.4
		8	68.6	78.6	11.5	7.5	2.4
	0.15	4	50.9	79.3	10.6	6.5	3.6
		5	58.9	78.5	12.6	6.6	2.3
		6	64.6	77.3	12.9	6.4	3.4
		7	72.2	78.9	12.8	6.1	2.2
		8	72.2	78.9	12.8	6.1	2.2
[PSCH ₂ TBZ-Cu]	0.1	4	48.6	71.5	17.8	7.7	3.1
		5	53.3	73.5	16.3	7.4	2.8
		6	55.4	72.2	16.5	8.9	2.4
		7	60.8	73.4	15.7	8.7	2.2
		8	60.8	73.4	15.7	8.7	2.2
	0.15	4	52.7	73.6	15.5	8.5	2.4
		5	55.1	74.7	14.6	7.3	3.4
		6	62.8	74.7	14.6	7.4	3.3
		7	64.8	73.8	15.4	8.3	2.5
		8	64.8	73.8	15.4	8.3	2.5

289 *Reaction conditions: CH₃CN (20 ml), ethylbenzene (10 mmol), TBHP (20 mmol), Temperature (65 °C); Conversion refers to 290 GCMS analysis.





292

293

Fig. 6(a-d). Study of time variation on ethylbenzene oxidation with immobilized catalysts

294

Catalyst reusability

295

A crucial aspect of heterogeneous catalysis is catalyst recyclability. After each reaction cycle, the catalysts were recovered, washed, and reused under identical conditions. From the **Table 6** and **Fig. 7**, it can be observed that, performance remained largely unchanged over three consecutive cycles, with only a slight decrease observed after the fourth cycle due to loss of metal content. Structural integrity was confirmed through spectroscopic analysis, and atomic absorption spectroscopy (AAS) revealed minimal metal leaching, ensuring the catalysts' stability.

302

Table 6. Recyclability Test

Catalyst	Cycle	Conversion (%)	Selectivity (%)			
			 -CHO	 -COO	 -COOH	Others
[PSCH ₂ -TBZ-V]	1	74.4	80.2	12.7	4.8	2.3
	2	74.4				
	3	74.4				
	4	74.1				
	5	72.2				
[PSCH ₂ -TBZ-Mn]	1	82.8	80.0	11.8	4.6	3.6
	2	82.8				
	3	82.8				
	4	82.5				
	5	79.2				
[PSCH ₂ -TBZ-Cu]	1	55.5	75.8	20.1	3.1	1.0
	2	55.5				
	3	55.5				
	4	55.1				
	5	52.2				

303 *Reaction conditions: CH₃CN (20 ml), Ethylbenzene (10 mmol), H₂O₂ (20 mmol), 0.15 gm catalyst,
304 Temperature (65 °C); Time (7 h) Conversion refers to GCMS analysis.

305

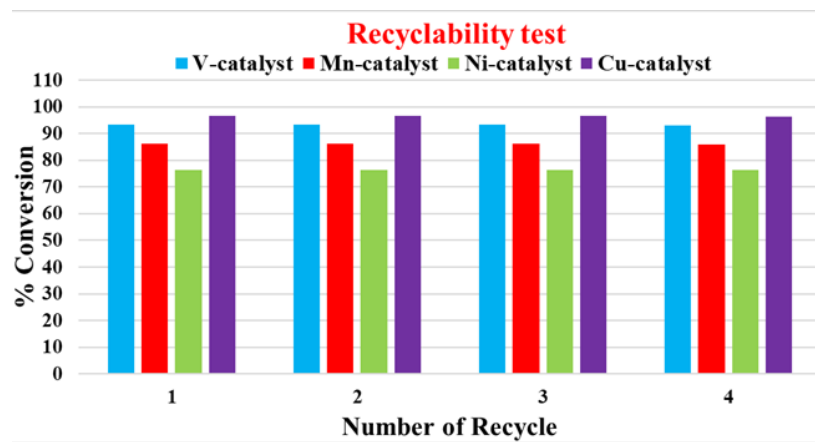
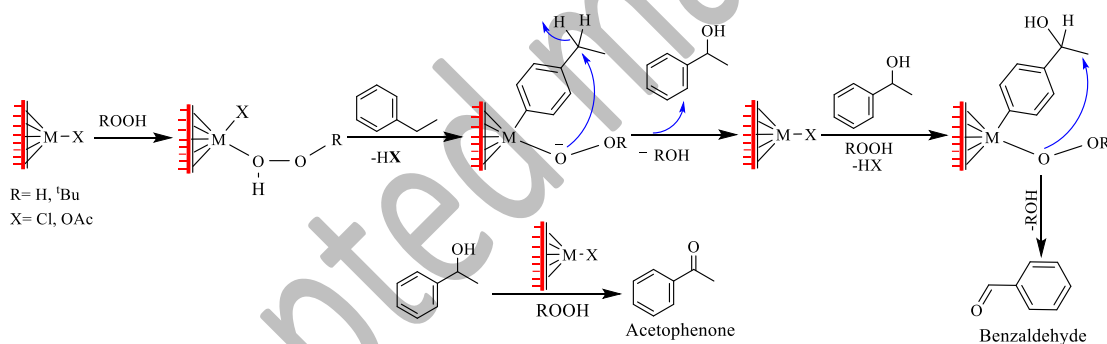


Fig. 7. Recycling performance of polystyrene-bound metal catalyst

Plausible Mechanism

Scheme 2 shows the mechanism [36] for the oxidation of ethylbenzene in presence peroxide ($\text{H}_2\text{O}_2/\text{TBHP}$) and catalyzed by metal catalyst. Firstly, metal catalyst in presence of peroxide forms active hydroperoxide species leaving out chloride ion/acetate ion. The benzylic carbocation is stabilized by resonance, allowing a nucleophilic attack by the *tert*-butylperoxide anion to generate phenyl ethanol which further undergoes rearrangement and cleavage of peroxide bond to yield benzaldehyde and acetophenone.



Scheme 2. Proposed mechanism for the $\text{H}_2\text{O}_2/\text{TBHP}$ mediated oxidation of ethylbenzene catalysed by supported metal catalyst

CONCLUSION

This study focuses on the synthesis and catalytic application of immobilized 2-(2-pyridyl)benzimidazole metal complexes for the efficient liquid phase oxidation of ethylbenzene. The catalysts were prepared by covalently anchoring 2-(2-pyridyl)benzimidazole onto a chloromethylated polystyrene support, followed by the incorporation of Cu^{II} , V^{IV} , and Mn^{II} metal ions. Under optimized reaction conditions (0.15 g catalyst, 65 °C, 7 h) and using hydrogen peroxide as an oxidant, the catalysts exhibited significant activity for ethylbenzene oxidation. Among the primary oxidation products-benzaldehyde, acetophenone, and phenylacetic acid,benzaldehyde was identified as the

327 most selectively formed product. The conversion efficiency and benzaldehyde selectivity in
328 the presence of H₂O₂ followed the order Mn (82.8%) > V (74.4%) > Cu (55.5%) and Mn
329 (82.5) > V (81.8) > Cu (76.5), respectively. When tert-butyl hydroperoxide (TBHP) was used
330 as the oxidant, the conversion rates and selectivity followed Mn (72.2%) > Cu (64.8%) > V
331 (55.6%) and Mn (80.3) > V(77.1) > Cu(74.7), respectively. Overall, the manganese-based
332 catalyst emerged as the most effective in terms of both conversion rate and selectivity. This
333 research underscores the potential of polymer-supported catalysts as efficient and reusable
334 systems for ethylbenzene oxidation. Further investigations could explore their application in
335 broader catalytic transformations while optimizing conditions for industrial scalability and
336 environmental sustainability.

337 **FUNDING**

338 This work was supported by ongoing institutional funding. No additional grants to carry out
339 or direct this particular research were obtained.

340 **CONFLICTS OF INTEREST**

341 The authors declare no conflict of interest.

REFERENCES

- 342 1. Rahman, M.M., Ara, M.G., Rahman, M.S., Uddin, M.S., Bin-Jumah, M.N., Abdel-Daim,
343 M.M. (2020). Recent development of catalytic materials for ethylbenzene
344 oxidation. *Journal of Nanomaterials*, **1**, 7532767. <https://doi.org/10.1155/2020/7532767>
- 345 2. Bäckvall, J.E. (Ed.). (2011). *Modern oxidation methods*. John Wiley & Sons.
- 346 3. He, C., Cheng, J., Zhang, X., Douthwaite, M., Pattisson, S., Hao, Z. (2019). Recent
347 advances in the catalytic oxidation of volatile organic compounds: a review based on
348 pollutant sorts and sources. *Chemical reviews*, **119**(7), 4471-4568.
349 <https://doi.org/10.1021/acs.chemrev.8b00408>
- 350 4. Poovan, F., Chandrashekhar, V.G., Natte, K., Jagadeesh, R.V. (2022). Synergy
351 between homogeneous and heterogeneous catalysis. *Catalysis Science &*
352 *Technology*, **12**(22), 6623. <https://doi.org/10.1039/D2CY00232A>
- 353 5. Khokhar, D., Kour, M., Phul, R., Sharma, A.K., Jadoun, S. (2024). Polystyrene-
354 supported Catalysts. In *Polymer Supported Organic Catalysts*, CRC Pres, pp. 89-100.
- 355 6. Kumari, S., Kumar, S., Karan, R., Bhatia, R., Kumar, A., Rawal, R.K., Gupta, P.K.
356 (2024). Synthetic and catalytic perspectives of polystyrene supported metal
357 catalyst. *Journal of the Iranian Chemical Society*, **21**(4), 951.
358 <https://doi.org/10.1007/s13738-024-02970-7>

359 7. Kargar, H., Moghadam, M., Shariati, L., Feizi, N. (2022). Novel oxo–peroxo W (VI) Schiff
360 base complex: Synthesis, SC-XRD, spectral characterization, supporting on
361 chloromethylated polystyrene, and catalytic oxidation of sulfides. *Journal of the Iranian
362 Chemical Society*, **19(7)**, 3067-3077. <https://doi.org/10.1007/s13738-022-02517-8>

363 8. Maurya, M.R., Patter, A., Chauhan, A., Kumar, N. (2024). Dioxidomolybdenum
364 (VI) Complex Supported on Chloromethylated Polymer and Its Catalytic Role in Peroxidase
365 Mimicking Activity Towards Oxidation of Dopamine. *Topics in Catalysis*, **67(5)**, 466-482.
366 <https://doi.org/10.1007/s11244-023-01861-0>

367 9. Sharma, A.S., Sharma, V.S., Yadav, P., Kaur, H., Varma, R.S. (2023). Polystyrene
368 Resins: Versatile and Economical Support for Heterogeneous Nanocatalysts in
369 Sustainable Organic Reactions. *ChemCatChem*, **15(8)**, e202201493.
370 <https://doi.org/10.1002/cctc.202201493>

371 10. Chakravarthy, A.J., Madhura, M.J., Gayathri, V. (2024). A Novel Polymer Supported
372 Copper (II) Complex as Reusable Catalyst in Oxidative Esterification. *Catalysis
373 Letters*, **154(2)**, 725. <https://doi.org/10.1007/s10562-023-04337-8>

374 11. Gautam, P., Shah, J.A., Bhanage, B.M. (2023). Palladium-Catalyzed Carbonylation
375 Reactions in Ionic Liquids. In *Encyclopedia of Ionic Liquids* (pp. 991-1004). Singapore:
376 Springer Nature Singapore. https://doi.org/10.1007/978-981-33-4221-7_32

377 12. Dehbanipour, Z., Moghadam, M., Tangestaninejad, S., Mirkhani, V., Mohammadpoor-
378 Baltork, I. (2022). An efficient and selective olefination of aldehydes with ethyl
379 diazoacetate using copper (II) bis-thiazole complex as heterogeneous catalyst. *Journal
380 of the Iranian Chemical Society*, **19(8)**, 3371. <https://doi.org/10.1007/s13738-022-02530-x>

382 13. Suzuki, N., Watanabe, K., Takahashi, C., Takeoka, Y., Rikukawa, M. (2023).
383 Ruthenium-catalyzed Olefin Metathesis in Water using Thermo-responsive Diblock
384 Copolymer Micelles, *Current Organic Chemistry*, **27(15)**, 1347.
385 <https://doi.org/10.2174/1385272827666230911115809>

386 14. Bakhvalova, E.S., Pinyukova, A.O., Mikheev, A.V., Demidenko, G.N., Sulman, M. G.,
387 Bykov, A.V., Kiwi-Minsker, L. (2021). Noble metal nanoparticles stabilized by hyper-
388 cross-linked polystyrene as effective catalysts in hydrogenation of
389 arenes. *Molecules*, **26(15)**, 4687. <https://doi.org/10.3390/molecules26154687>

390 15. Rajmane, A., Mahey, J., Kamble, S., Kumbhar, A. (2024). In Situ generated PdNPs
391 immobilized on polystyrene supported DABCO Dicationic ionic liquid: An efficient and
392 reusable catalyst for Suzuki and Heck coupling reactions. *J. Organomet. Chem.*, **1022**,
393 123390. <https://doi.org/10.1016/j.jorgancchem.2024.123390>

394 16. Chkirate, K., Essassi, E.M. (2022). Pyrazole and benzimidazole derivatives: chelating
395 properties towards metals ions and their applications. *Current Organic*
396 *Chemistry*, **26(19)**, 1735. <https://doi.org/10.2174/138527282766221216110504>

397 17. Singha, D., Halder, S.C., Jana, A.D., Pal, N. (2024). The coordination chemistry and
398 supramolecular interactions of 2-(2'-Pyridyl)imidazole ligand: a comprehensive review
399 with theoretical insight. *Reviews in Inorganic Chemistry*, **44(2)**, 231.
400 <https://doi.org/10.1515/revic-2023-0016>

401 18. Maurya, M.R., Arya, A., Adao, P., Pessoa, J.C. (2008). Immobilisation of oxovanadium
402 (IV), dioxomolybdenum (VI) and copper (II) complexes on polymers for the oxidation of
403 styrene, cyclohexene and ethylbenzene. *Applied Catalysis A: General*, **351(2)**, 239.
404 <https://doi.org/10.1016/j.apcata.2008.09.021>

405 19. Renuka Maldepalli, K., Virupaiah, G. (2017). A polymer-anchored cobalt (II) complex as
406 a reusable catalyst for oxidation of benzene, ethylbenzene and cyclohexane. *Trans.*
407 *Met. Chem.*, **42**, 25. <https://doi.org/10.1007/s11243-016-0102-z>

408 20. Opgrande, J.L., Dobratz, C.J., Brown, E., Liang, J., Conn, G.S., Shelton, F.J., With, J.
409 (2000). Benzaldehyde. *Kirk-Othmer Encyclopedia of Chemical Technology*.
410 <https://doi.org/10.1002/0471238961.0205142615160718.a01>

411 21. Zubkov, F.I., Kouznetsov, V.V. (2023). Traveling across life sciences with acetophenone
412 a simple ketone that has special multipurpose missions. *Molecules*, **28(1)**, 370.
413 <https://doi.org/10.3390/molecules28010370>

414 22. Cook, S. D. (2019). An historical review of phenylacetic acid. *Plant and Cell*
415 *Physiology*, **60(2)**, 243. <https://doi.org/10.1093/pcp/pcz004>

416 23. Khalil M. M. H. (2000). $M(CO)_4[2-(2'-pyridyl) benzimidazole]$ complexes; $M = Mo$ or W .
417 *Trans. Met. Chem.*, **25(3)**, 358–360. <https://doi:10.1023/a:1007001003628>

418 24. Tuna M., Ugur T. (2022). Synthesis of novel of Mn (II), Co (II), and Cu (II) Schiff base
419 complexes and their high catalytic effect on bleaching performance with H_2O_2 . *J. Mol.*
420 *Struct.* **1265**, 133348. <https://doi.org/10.1016/j.molstruc.2022.133348>

421 25. Sharma B. P., Subin J. A., Marasini B. P., Adhikari R., Pandey S. K., Sharma M. L.,
422 (2023) Triazole based Schiff bases and their oxovanadium(IV) complexes: Synthesis,
423 characterization, antibacterial assay, and computational assessments. *Helion. 9(4)*, 1.
424 <https://doi.org/10.1016/j.heliyon.2023.e15239>

425 26. Singh V. P., Singh S., Katiyar A. (2009). Synthesis, physico-chemical studies of
426 manganese (II), cobalt (II), nickel (II), copper (II) and zinc (II) complexes with some p-
427 substituted acetophenone benzoylhydrazones and their antimicrobial activity. *J.*
428 *Enzyme Inhib. Med. Chem.*, **24(2)**, 577. <https://doi:10.1080/14756360802318662>

429 27. Sahani M.K., Yadava U., Pandey O.P., Sengupta S.K. (2014) *Spectrochim. Acta A Mol.*
430 *Biomol. Spectrosc.*, **125**, 189. <https://doi:10.1016/j.saa.2014.01.041>

431 28. Renuka, M.K., Gayathri, V. (2019) Oxidation of Benzyl Alcohols by Polymer Supported
432 V(IV) Complex Using O₂. *Catal. Lett.* **149**, 1266–1276. <https://doi.org/10.1007/s10562-019-02710-0>

433 29. Lupaşcu G., Pahonțu E., Shova S., Bărbuceanu, Ștefania F., Badea M., Paraschivescu
434 C., DinuPîrvu C. E., (2021). Co (II), Cu (II), Mn (II), Ni (II), Pd (II), and Pt (II) complexes
435 of bidentate Schiff base ligand: Synthesis, crystal structure, and acute toxicity
436 evaluation. *Appl. Organomet. Chem.*, **35**(4), 1. <https://doi.org/10.1002/aoc.6149>

437 30. Chandra S., Gupta L.K., (2004) EPR, IR and electronic spectral studies on Mn(II), Co(II),
438 Ni(II) and Cu(II) complexes with a new 22-membered azamacrocyclic [N₄] ligand.
439 *Spectrochimica Acta Part A: Molecular and Biomolecular Spectroscopy* **60**(8-9), 1751-
440 1761. <https://doi.org/10.1016/j.saa.2003.07.011>

441 31. Singh Y.P., Patel R.N., Singh Y., Butcher R.J., Vishakarma P.K., Singh R.K.B. (2016).
442 Structure and antioxidant superoxide dismutase activity of copper (II) hydrazone
443 complexes, *Polyhedron*. **122**(28), 1-15. <http://dx.doi.org/10.1016/j.poly.2016.11.013>

444 32. Krzystek, J., Ozarowski, A., Telser, J., & Crans, D.C. (2015). High-frequency and -field
445 electron paramagnetic resonance of vanadium (IV, III, and II) complexes. *Coord. Chem.*
446 *Rev.*, 301-302, 123–133. <https://doi:10.1016/j.ccr.2014.10.014>

447 33. Mahboubi-Anarjan P., Bikas R., Hosseini-Monfared H., Aleshkevych P., Mayer P. (2017)
448 Synthesis, characterization, EPR spectroscopy and catalytic activity of a new
449 oxidovanadium (IV) complex with N₂O₂-donor ligand. *J. Mol. Struct.* **1131** 258-265.
450 <https://doi.org/10.1016/j.molstruc.2016.11.059>

451 34. Hachuła, B., Pędras, M., Nowak, M., Kusz, J., Skrzypek, D., Borek, J., Pentak, D.
452 (2009). Synthesis, crystal structure, spectroscopic, and magnetic properties of a
453 manganese (II) methoxyacetate complex [Mn(C₆O₆H₁₀)(H₂O)]_n. *J. Coord. Chem.*, **63**(1),
454 67. <https://doi:10.1080/0095897090315535>

455 35. Ali I.O., Nassar H.S., El-Nasser K.S., Bougarech A., Abid, M., Elhenawy, A.A., (2021)
456 Synthesis and characterization of Mn (II) and Co(II) complexes with poly(vinyl alcohol-
457 nicotinic acid) for photocatalytic degradation of Indigo carmine dye. *Inorg Chem*
458 *Commun.* **124**, 108360. <https://doi.org/10.1016/j.inoche.2020.108360>

459 36. Azeez M.O., Nafiu S.A., Olarewaju T.A., Olabintan A.B., Tanimu A., Gambo Y., Aitani
460 A. (2023). Selective Catalytic Oxidation of Ethylbenzene to Acetophenone: A Review of
461 Catalyst Systems and Reaction Mechanisms. *Ind. Eng. Chem. Res.*, **62**(33), 1.
462 <https://doi.org/10.1021/acs.iecr.3c01588>

463